5‘ → 3‘ Molecular Polarity of Human Replication Protein A (hRPA) Binding to Pseudo-Origin DNA Substrates †

ARTICLE *in* BIOCHEMISTRY · NOVEMBER 2000

Impact Factor: 3.02 · DOI: 10.1021/bi0005761 · Source: PubMed

2 AUTHORS:

Cristina Iftode
Rowan University
15 PUBLICATIONS **445** CITATIONS
SEE PROFILE

James A Borowiec
NYU Langone Medical Center
45 PUBLICATIONS **3,275** CITATIONS
SEE PROFILE

5′ → 3′ Molecular Polarity of Human Replication Protein A (hRPA) Binding to Pseudo-Origin DNA Substrates[†]

Cristina Iftode[‡] and James A. Borowiec*

Department of Biochemistry and Kaplan Comprehensive Cancer Center, New York University School of Medicine, 550 First Avenue, New York, New York 10016

Received March 13, 2000; Revised Manuscript Received June 23, 2000

ABSTRACT: Human replication protein A (hRPA) was previously seen to efficiently bind a 48 bp simian virus 40 (SV40) "pseudo-origin" (PO) substrate that mimics a DNA structure found within the SV40 T antigen−origin (*ori*) complex. To understand the role of hRPA during the initiation of replication, we examined the PO sequence and structure requirements for hRPA interaction. Binding and unwinding were found to be most efficient when both strands of the central 8 nt single-stranded DNA (ssDNA) bubble region contained a polypyrimidine structure, with these activities proportionately reduced when the bubble region was replaced with a purine tract on one or both strands. Examination of the importance of the two duplex flanks indicates that the early gene side contains a DNA structural feature located one duplex turn from the bubble whose mutation significantly affects the affinity of hRPA for the substrate. When present in the context of *ori*, mutation of this sequence was seen to have significant effects on SV40 DNA replication in vitro and on the denaturation of *ori*, indicating that origin activity can be modulated by cis-acting elements which alter the hRPA binding affinity. Use of fork and overhang substrates containing 8 nt pyrimidine or purine arms demonstrates that hRPA binding to DNA involves a particular molecular polarity in which initial hRPA binding occurs on the 5′ side of a ssDNA substrate, and then extends in the 3′ direction to create a stably bound hRPA. These data have implications on the mechanism of the initiation of eukaryotic DNA replication as well as on the sites of nascent strand synthesis within the origin.

The initiation of DNA replication from an internal site on duplex DNA requires formation of an incipient replication bubble, and the extension of this bubble to facilitate entry of the replication machinery. In various prokaryotic and eukaryotic DNA replication systems, the cognate single-stranded DNA-binding protein (SSB) plays a critical role in the formation of the large replication bubble (*1*−*4*). Although one of the key roles of the SSB is to prevent reannealing of the denatured origin region, recent evidence from the simian virus 40 (SV40) replication system indicates that the host SSB, the heterotrimeric replication protein A (RPA) (*5*), also plays an important dynamic role in origin denaturation (*6*, *7*). However, the mechanistic role of RPA in this process remains unclear.

The SV40 origin (*ori*) contains three elements shown by mutational analysis to be important for the initiation of DNA replication in vivo and in vitro (*8*−*11*). From the early to late gene sides of *ori*, these domains are an imperfect inverted repeat termed the early palindrome (EP), a central 27 bp dyad symmetry element containing four 5′-GAGGC-3′ sequence repeats that serve as recognition elements for binding of the viral large tumor antigen (T antigen), and an AT-rich (AT) element. The initiation of SV40 DNA replication entails the ATP-dependent formation of a T antigen double hexamer over *ori* (*12*−*16*). Formation of this ATP-dependent complex induces the melting of an 8 bp region within the EP (*17*, *18*), and causes distortion of the AT element. The addition of human RPA (hRPA) or RPA from *Saccharomyces cerevisiae* (scRPA) to the T antigen−*ori* complex causes denaturation of *ori*, releasing the T antigen DNA helicase to unwind the viral chromosome (*3*, *4*, *19*−*24*). Current evidence indicates that hRPA binding to the 8 nt single-stranded DNA (ssDNA) bubble is a key step in the *ori* denaturation reaction (*6*, *7*). Use of 48 bp pseudo-origin (PO) substrates that contain a central 8 nt bubble in the context of the *ori* sequence demonstrates that hRPA can recognize these substrates using a combination of contacts with the ssDNA bubble and the duplex flanks (*6*, *7*, *25*). hRPA binding to the PO substrate generates structural distortion to each duplex flank and, on a fraction of the bound substrate pool, induces substrate denaturation (*6*, *7*).

hRPA binding to ssDNA has been postulated to occur in a two-step pathway in which hRPA first binds 8 nt unstably (to form the $hRPA_{8nt}$ complex) (*26*−*28*). hRPA then undergoes a conformational transition causing hRPA to bind stably and occlude 30 nt (the $hRPA_{30nt}$ complex) (*26*, *27*, *29*−*32*). Denaturation of the PO substrates likely proceeds by a similar route in which hRPA initially interacts with the 8 nt bubble using the $hRPA_{8nt}$ complex. In a step facilitated by a transition to the $hRPA_{30nt}$ complex, hRPA destabilizes the duplex flanks to extend the bubble and denature the substrate (*6*, *7*). hRPA binding in the two complexes may involve

[†] This research was supported by NIH Grant AI29963 and Kaplan Cancer Center Developmental Funding and a Kaplan Cancer Center Support Core Grant (NCI P30CA16087).

* To whom correspondence should be addressed. Phone: (212) 263-8453. Fax: (212) 263-8166. E-mail: James.Borowiec@med.nyu.edu.

[‡] Present address: Department of Molecular Biology, Lewis Thomas Laboratory, Princeton University, Princeton, NJ 08544.

10.1021/bi0005761 CCC: $19.00
Published on Web 08/31/2000

different usage of the four DNA-binding domains (DBDs) identified within hRPA and scRPA. Structural and mutational analyses of hRPA and scRPA indicate that two highly similar DNA-binding domains (DBDs A and B) are located in tandem in the center of the large RPA subunit which yield a high-affinity DNA binding site capable of interacting with 8 nt of ssDNA (*33*−*37*). Two secondary DBDs are located in the C-terminus of the large subunit (DBD C) (*25*, *38*), and in the center of the middle RPA subunit (DBD D) (*36*, *39*, *40*).

To further understand the involvement of RPA in the initiation of eukaryotic DNA replication, we examined the DNA structure requirements for hRPA binding to the PO substrates. These data indicate that the affinity of hRPA is significantly modulated by the sequence of both the ssDNA and duplex DNA (dsDNA) portions of the PO molecule. In addition, our data reveal that hRPA binding to the PO substrate involves molecular polarity of the protein with the initial binding to the 8 nt bubble subsequently extended in the 5′ → 3′ direction to yield the $hRPA_{30nt}$ complex.

EXPERIMENTAL PROCEDURES

Protein Purification and Replication Extracts. Recombinant hRPA was expressed in and purified from *Escherichia coli* as described by Henricksen et al. (*41*), as modified by Iftode and Borowiec (*7*). The SV40 large T antigen was immunoaffinity purified from Sf9 insect cells infected with recombinant baculovirus as described by Borowiec (*42*).

To prepare extracts competent for SV40 DNA replication in vitro, mid-log HeLa cells (4×10^{10} cells) were harvested and washed as described by Wobbe et al. (*43*). Cells were swollen in 3 volumes of 20 mM HEPES (pH 7.5), 5 mM NaCl, 1.5 mM EDTA, and 1 mM DTT and lysed with a dounce homogenizer (15 strokes using a B pestle). After adjustment to 200 mM NaCl, the lysate was centrifuged at 50000*g* for 30 min at 4 °C and dialyzed against 20 mM HEPES (pH 7.5), 1 mM DTT, 0.1 mM EDTA, 10% glycerol, and 50 mM NaCl. Following dialysis, the extract was clarified by centrifugation at 15000*g* (30 min at 4 °C).

Preparation of Pseudo-Origin Substrates and Their Derivatives. *(1) Bubble Sequence Variants*. The PO-8 molecule, a 48 bp DNA molecule containing a central 8 nt ssDNA region, was prepared by annealing two partially complementary oligonucleotides [DNAgency (Malvern, PA) and Oligos Etc. (Bethel, ME)] as described previously (*6*). The top and bottom strand PO-8 sequences were as follows (ssDNA regions underlined): top, 5′-AGG CCT CCA AAA AAG CCT CCT CAC TAC TTC TGG AAT AGC TCA GAG GCC; bottom, 5′-GGC CTC TGA GCT ATT CCA GAT CAT CAC TGG AGG CTT TTT TGG AGG CCT. Four variants, differing only in the ssDNA bubble sequence (see Figure 1), were similarly prepared. The bubble region sequence of these variants is as follows: Pyr/Pyr-bubble substrate, T_8 on both strands; Pur/Pur-bubble substrate, A_8 on both strands; Pur/Pyr-bubble substrate, A_8 on the top strand and C_8 on the bottom strand; Pyr/Pur-bubble substrate, C_8 on the top strand and A_8 on the bottom strand.

(2) Fork Variants. Partially complementary oligonucleotides were annealed to generate substrates with fork or overhang structures (see Figure 3). Named by the sequence of the ssDNA arms, the fork substrates had differing 8 nt ssDNA extensions located toward the early gene (left) side of 40 bp of duplex DNA. The duplex DNA, identical in all the variants, was composed of SV40 origin sequence with the leftward 20 bp identical to that found in the rightward flank of the PO-8 bubble substrate (SV40 positions 5218 to 5237; see above). The additional 20 bp of duplex DNA in the fork substrate continues the natural SV40 origin sequence (SV40 positions 5238 to 14). The PO-8 fork substrate (whose top and bottom strand ssDNA sequences were identical to those found in the PO-8 bubble substrate) was constructed from the following two oligonucleotides (ssDNA extensions are underlined): top strand, 5′-TCA CTA CTT CTG GAA TAG CTC AGA GGC CGA GGC GGC CTC GGC CTC TGC-3′; bottom strand, 5′-GCA GAG GCC GAG GCC GCC TCG GCC TCT GAG CTA TTC CAG ATC ATC ACT-3′. Two fork variants were constructed that differed only in the sequence of the ssDNA arms. The sequence of these arms was as follows: Pyr/Pur-fork, C_8 on the top strand and A_8 on the bottom strand; Pur/Pyr-fork, A_8 on the top strand and C_8 on the bottom strand. Two overhang substrates were prepared that contained a ssDNA extension on only one of the two strands: 5′-Pyr-overhang, C_8 on the top strand; 3′-Pyr-overhang, C_8 on the bottom strand.

(3) Palindromic and Inverse Substrates. Synthetic oligonucleotides were designed to generate, after annealing, four 48 nt palindromic or "inverse" substrates. As depicted (see Figure 5), two substrates were constructed in which the early (Early-Pal substrate) or late (Late-Pal substrate) flank of the PO-8 bubble substrate was duplicated to yield a substrate with 2-fold symmetry. To avoid self-annealing of individual strands, the palindromic sequences contained base substitu-

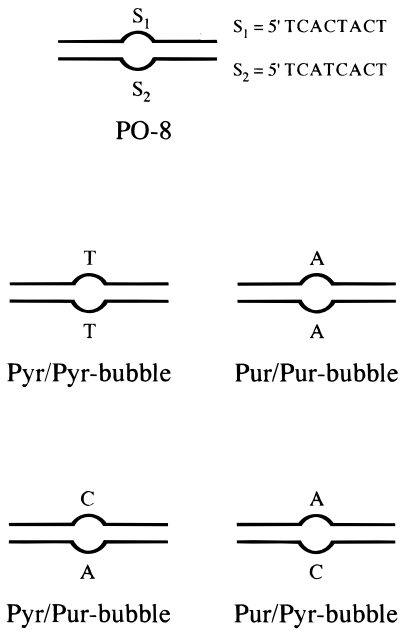

FIGURE 1: Pseudo-origin molecules used to test the bubble sequence requirements for substrate binding and unwinding by hRPA. In addition to the PO-8 control, four SV40 PO substrates containing 8 nt bubbles with a different content of pyrimidines and purines were constructed. The Pyr/Pyr-bubble molecule has a T_8 element on both strands of the bubble, while the Pur/Pur-bubble substrate contains an A_8 tract on both bubble strands. The Pyr/Pur-bubble substrate has a bubble composed of cytosines (C_8) on the top strand and adenines (A_8) on the bottom strand, while this orientation is reversed for the Pur/Pyr-bubble. The modified bubbles are flanked by PO-8 duplex sequences.

tions at two top strand positions: Early-Pal, G to A substitutions at positions 33 and 41; Late-Pal, a G to C substitution at position 33 and an A to T substitution at position 44. These substrates (and the inverse substrates described below) were constructed with the PO-8 bubble region. The palindromic molecules have the following sequence (with the replaced PO-8 sequences underlined and the ssDNA sequence shown in bold): Early-Pal, 5′-AGG CCT CCA AAA AAG CCT CC**T CAC TAC T**GG AGA CTT TTT TAG AGG CCT-3′ (top strand) and 5′-AGG CCT CTA AAA AAG TCT CC**T CAT CAC T**GG AGG CTT TTT TGG AGG CCT-3′ (bottom strand); Late-Pal, 5′-GGC CTC TGA GCT ATT CCA GA**T CAC TAC T**TC TGC AAT AGC TCA GTG GCC-3′ (top strand) and 5′-GGC CAC TGA GCT ATT GCA GA**T CAT CAC T**TC TGG AAT AGC TCA GAG GCC-3′ (bottom strand).

Two other inverse substrates were prepared: the Early-Inv substrate, in which the late flank sequence was replaced with the mirror image of the early flank, and the Late-Inv substrate, in which the early flank was replaced with the mirror image of the late flank (see Figure 5 and Results). The inverse substrates have the following sequence (with the replaced PO-8 sequences underlined and the ssDNA sequence shown in bold): Early-Inv, 5′-AGG CCT CCA AAA AAG CCT CC**T CAC TAC T**CC TCC GAA AAA ACC TCC GGA-3′ (top strand) and 5′-TCC GGA GGT TTT TTC GGA GG**T CAT CAC T**GG AGG CTT TTT TGG AGG CCT-3′ (bottom strand); Late-Inv, 5′-CCG GAG ACT CGA TAA GGT CT**T CAC TAC T**TC TGG AAT AGC TCA GAG GCC-3′ (top strand) and 5′-GGC CTC TGA GCT ATT CCA GA**T CAT CAC T**AG ACC TTA TCG AGT CTC CGG-3′ (bottom strand).

(4) Bending Derivatives. To construct the PO-8 bending variants (see Figure 7), the sequence of the PO-8 bubble region and late duplex flank was retained for each substrate. The sequence of the bending substrates is as follows (with the mutated PO-8 sequences underlined and the ssDNA sequence shown in bold): TA-bend, 5′-AGG CCT CCT TTT TTG CCT CC**T CAC TAC T**TC TGG AAT AGC TCA GAG GCC-3′ (top strand) and 5′-GGC CTC TGA GCT ATT CCA GA**T CAT CAC T**GG AGG CAA AAA AGG AGG CCT-3′ (bottom strand). For the following substrates, only the sequence of the early gene (left) side is shown (the mutated PO-8 sequences are underlined): GC-bend, 5′-AGG CCT CCG GGC CCG CCT CC...-3′ (top strand) and 5′-...GGA GGC GGG CCC GGA GGC CT-3′ (bottom strand); CG-bend, 5′-AGG CCT CCC CCG GGG CCT CC...-3′ (top strand) and 5′-...GGA GGC CCC GGG GGA GGC CT-3′ (bottom strand).

Construction of Plasmids. Plasmids containing either the wild-type (pBS-ATwt) or mutated (pBS-ATmt, pBS-TAmt, pBS-GCmt, and pBS-CGmt) SV40 origins were constructed by subcloning 90 bp fragments (positions 5186 to 32) into the *Bam*HI and *Xho*I sites of pBluescript SK+ phagemid (Stratagene). All inserts were made de novo by annealing synthetic oligonucleotides. The sequence of the wild-type origin is as follows: top strand, 5′-GAT CCG CCT AGG CCT CC**A AAA AA**G CCT CCT CAC TAC TTC TGG AAT AGC TCA GAG GCC GAG GCG GCC TCG GCC TCT GCA TAA ATA AAA AAA ATT AGC-3′; bottom strand, 5′-TCG AGC TAA TTT TTT TTA TTT ATG CAG AGG CCG AGG CCG CCT CGG CCT CTG AGC TAT TCC AGA AGT AGT GAG GAG GCT TTT TTG GAG GCC TAG GCG-3′. All mutant origins have CC (underlined) to AT substitutions at positions 5193 and 5194 and CT (underlined) to TA substitutions at positions 5206 and 5207 (to prevent T antigen binding to binding site I; see Results). The wild-type sequence between positions 5198 and 5203 (in bold) was replaced in the mutant origins (with the exception of pBS-ATmt, where this sequence was kept the same) with the following sequences: pBS-TAmt, TTTTTT; pBS-GCmt, GGGCCC; pBS-CGmt, CCCGGG. The identity of the plasmids was confirmed by sequencing of the inserts (Skirball Institute Sequencing Facility).

Gel Shift Analysis of hRPA Binding Reactions. Standard reaction mixtures (20 μL) containing hRPA (0.01−6 pmol), 5′-^{32}P-labeled DNA substrates (0.05−1.5 pmol), 30 mM HEPES (pH 7.8), 7 mM $MgCl_2$, 0.5 mM DTT, and 2 μg of bovine serum albumin were incubated for 20 min at 37 °C. To cross-link the hRPA−DNA complexes, glutaraldehyde was subsequently added to a final concentration of 0.1%, and the reaction mixture was incubated for an additional 15 min. Protein−DNA complexes were separated by 5% native polyacrylamide (29:1 acrylamide:bisacrylamide ratio) gel electrophoresis at 8 V/cm using 45 mM Tris (pH 7.5), 45 mM boric acid, and 1 mM EDTA as the running buffer. The hRPA−DNA complexes were visualized by autoradiography. The level of complex formation (or ssDNA for substrate unwinding experiments, below) was quantitated by densitometric analysis of digitized images using NIH Image (version 1.61) software.

Substrate Unwinding Reactions. Binding reactions, in the absence of glutaraldehyde, were carried out as described previously (*7*). To detect ssDNA generated as a result of unwinding by hRPA, reaction mixtures were extracted with a phenol/chloroform mixture (v/v; 1:1) in the presence of a 10-fold molar excess of unlabeled top strand (to reduce the level of reannealing of the labeled top strand) (*7*). The DNA samples were then separated on 8% nondenaturing polyacrylamide gels (29:1 acrylamide:bisacrylamide ratio) and subjected to autoradiography.

SV40 Ori Denaturation Reactions. *Ori* denaturation reaction mixtures (20 μL) containing 40 mM creatine phosphate (di-Tris salt, pH 7.8), 7 mM $MgCl_2$, 4 mM ATP, 0.5 mM DTT, 25 μg/mL creatine kinase, 1.0 μg of T antigen, 250 ng of either hRPA or *E. coli* SSB (EcoSSB), and 100 fmol of the appropriate 5′-^{32}P-labeled DNA substrate [∼210 bp, prepared by PCR amplification (*44*)] were incubated for 1.5 h at 37 °C. Reaction products were extracted with a phenol/chloroform mixture (v/v; 1:1) and then separated by electrophoresis through an 8% nondenaturing polyacrylamide gel (29:1 acrylamide:bisacrylamide ratio), and the reaction products were visualized by autoradiography.

SV40 DNA Replication Reactions. Standard reaction mixtures (30 μL) containing 30 mM HEPES (pH 7.5), 7 mM $MgCl_2$, 4 mM ATP, 40 mM creatine phosphate, 25 μg/mL creatine kinase, 0.4 mM DTT, CTP, GTP, and UTP (200 μM each), dATP, dGTP, and dCTP (100 μM each), 20 μM [^{3}H]dTTP (1−10 cpm/fmol; Amersham), 0.2 μg of the *ori*-containing plasmid (either pBS-ATwt, pBS-ATmt, pBS-TAmt, pBS-GCmt, or pBS-CGmt), 350 μg of HeLa replication extract, and 750 ng of SV40 T antigen were incubated at 37 °C for 2 h. To determine replication activity, the high-molecular weight DNA was precipitated with trichloroacetic

acid. The amount of ^3H in the precipitate was determined by scintillation counting.

RESULTS

Effect of ssDNA Bubble Sequence Composition on Binding and Denaturation of Pseudo-Origin Substrates. We previously observed that hRPA could bind and unwind an SV40 pseudo-origin substrate (PO-8) (*6*, *7*). This 48 bp molecule is essentially composed of SV40 *ori* region sequences centered around the 8 bp EP region that is found melted within the ATP-dependent T antigen−*ori* complex (*17*, *18*). To generate an 8 bp single-stranded region in the center of the substrate, the bottom strand oligonucleotide was designed to have the identical bases as those found on the opposite strand over this region. The substrate thus closely resembles the DNA structure generated by T antigen, and can be used to examine the role of hRPA in the *ori* denaturation reaction that occurs when hRPA is added to the T antigen−*ori* complex. Note that because heterologous SSBs (e.g., EcoSSB) (*45*) can replace hRPA in this reaction, specific contacts between hRPA and T antigen are not required for *ori* denaturation. The substrate can thus be reasonably expected to provide information concerning the specific role of hRPA in *ori* denaturation, because effects of T antigen on this step are eliminated.

We examined the ssDNA and duplex sequence composition requirements for hRPA binding to and unwinding of PO molecules. We first tested the effect on hRPA binding of altering the base composition of the PO-8 ssDNA bubble. The binding of hRPA was tested to PO-8 and to four PO-8 variants that differed only in the ssDNA sequence. The four variants had a pyrimidine tract (T_8) on both strands (the Pyr/Pyr-bubble), a purine tract (A_8) on both strands (the Pur/Pur-bubble), a pyrimidine tract (C_8) on the top strand and a purine tract (A_8) on the bottom strand (the Pyr/Pur-bubble), or a purine tract (A_8) on the top strand and a pyrimidine tract (C_8) on the bottom strand (the Pur/Pyr-bubble, Figure 1).

hRPA bound the Pyr/Pyr-bubble substrate with an affinity and stoichiometry similar to those for PO-8 (Figure 2A, lanes 2 and 6). In contrast, significant binding to the Pur/Pur-bubble substrate was not detected (lane 4). These results are consistent with previous findings showing a preferential association of hRPA with pyrimidine-rich ssDNA (*29*). However, because hRPA appears to initially associate with ssDNA unstably using an 8 nt binding site (*26*, *27*, *46*), our data indicate that DNA sequence composition can specifically modulate the affinity of hRPA for ssDNA during this first stage of binding. These data also demonstrate that the bubble sequence composition is a critical determinant for recognition of the PO substrates by hRPA.

The affinity of hRPA for the two mixed bubble substrates differed significantly with the apparent binding affinity for the Pyr/Pur- and Pur/Pyr-bubble substrates being ~38 and 11% of that of PO-8, respectively (by densitometric analysis; Figure 2A, lanes 8 and 10, respectively). Furthermore, while hRPA formed almost no trimers on the Pur/Pyr-bubble substrate (lane 10), the stoichiometry of hRPA binding to the Pyr/Pur-bubble substrate was identical to that of PO-8 (hRPA dimers and trimers are predominant) (compare lanes 2 and 8). This result is unexpected as equivalent hRPA

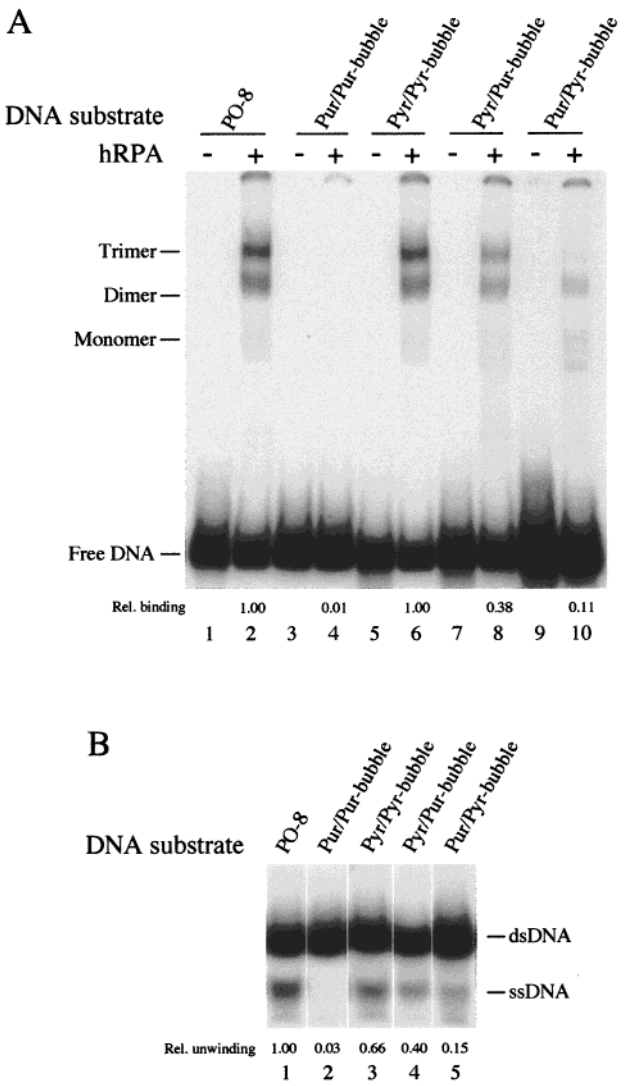

FIGURE 2: hRPA more efficiently binds and unwinds pseudo-origin substrates containing pyrimidine bubbles than purine bubbles. Each pseudo-origin substrate (5′-^{32}P-labeled; 0.15 pmol) was incubated in the presence or absence of 1.5 pmol of hRPA under standard binding (A) and unwinding (B) reaction conditions. The positions of hRPA multimers, generated ssDNA, and unbound and unwound substrate are indicated. The amount of substrate binding or unwinding was quantitated by digitization of images using Adobe Photoshop 4.0, and densitometric analysis of these images by NIH Image. The relative amount of substrate binding or unwinding is indicated below the appropriate lanes of panel A or B, respectively. Note that the stoichiometry of the hRPA complexes was determined in previous studies (*6*, *27*).

binding to the Pyr/Pur- or Pur/Pyr-bubble molecules would be predicted on the basis of the identical (albeit reversed) nucleotide composition of the bubble elements on each substrate. These data therefore implicate the sequence of the flanking duplex DNA as an important determinant affecting the efficiency of hRPA binding to the PO-8 molecule, a point addressed in greater detail below.

The unwinding activity of hRPA on these substrates paralleled binding (Figure 2B). The amount of ssDNA generated upon hRPA binding to the Pyr/Pyr-bubble substrate was slightly reduced from that produced on PO-8 (lanes 1 and 3). An intermediate unwinding level was observed with the Pyr/Pur-bubble substrate (lane 4), while very little (lane 5) or no unwinding (lane 2) was detected with the Pur/Pyr- or Pur/Pur-bubble substrate, respectively. Thus, these results

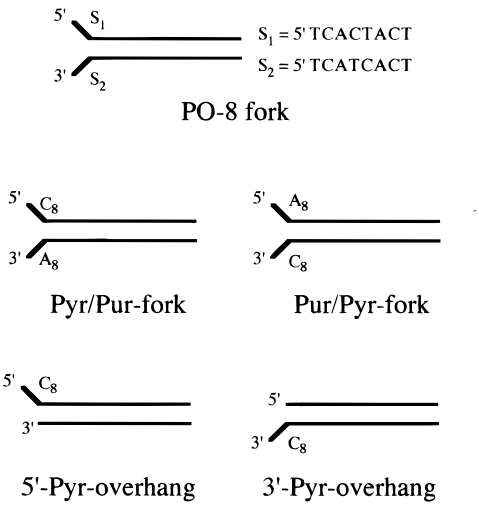

FIGURE 3: DNA substrates used to test the molecular polarity of hRPA binding. The polarity of pseudo-origin binding by hRPA was tested with both forklike and overhang substrates. The fork substrates were designed to have 8 nt arms located on the early gene side of the molecule. The PO-8 fork contains arms that have sequences that are identical to that found in the ssDNA region of the PO-8 bubble substrate (see Figure 1). The Pyr/Pur-fork contains cytosines (C_8) on the top and adenines (A_8) on the bottom arm, while the Pur/Pyr-fork has the opposite arm sequence. The duplex flanks located to the late gene side of the DNA molecules are composed of 20 bp of the late PO-8 flank followed by an additional 20 bp of the SV40 *ori* sequence (see Experimental Procedures). The overhang substrates contain a C_8 arm which extends to the early side of the molecule on either the top (5′-Pyr-overhang) or bottom (3′-Pyr-overhang) strand. The overhang substrates have a duplex sequence identical to that of the fork substrates.

reiterate earlier observations showing that relatively high-affinity binding by hRPA is a prerequisite of efficient pseudo-origin unwinding (*6*, *7*).

hRPA Binds Forklike Pseudo-Origin Substrates with a 5′ → 3′ Polarity. Previous observations reporting different hRPA binding modes and multiple DBDs within hRPA (*26*, *27*, *36*−*39*) suggest that hRPA binds ssDNA with a certain polarity. For example, we have previously postulated that hRPA initially binds ssDNA unstably using an 8 nt binding mode, and this binding is then stabilized by hRPA undergoing a conformational change to occlude 30 nt. Thus, hRPA may first contact 8 nt of ssDNA, and then extend this binding in the 5′ or 3′ direction.

Because the PO-8 substrate constrains the initial interaction of hRPA with ssDNA, the polarity of hRPA binding can be tested by using PO substrates with the bubble placed at one end of the DNA molecule. We therefore constructed two forklike substrates (48 bp) by removing the left duplex flank of the PO-8 substrate, yielding a fork structure on the left end of the molecule (Figure 3). The remaining right duplex flank of PO-8 was extended by the addition of 20 bp of SV40 origin sequence. For the Pyr/Pur-fork, the top and bottom strand fork arms contained pyrimidine (C_8) and purine (A_8) tracts, respectively. This orientation was reversed for the Pur/Pyr-fork. In addition, we designed two overhang substrates by removing either the bottom arm of the Pyr/Pur-fork (to create the 5′-Pyr-overhang) or the top arm of the Pur/Pyr-fork (yielding the 3′-Pyr-overhang substrate).

These four substrates should allow reasonable distinction between the ability of hRPA to bind ssDNA with a 5′ → 3′ or 3′ → 5′ polarity. From the experiments in which different bubble sequences were tested (i.e., Figure 2), we expect that the affinity of hRPA for the C_8 arm would be significantly higher than for the A_8 arm. Therefore, if hRPA bound DNA with a 5′ → 3′ molecular polarity, the initial hRPA contact with 8 nt of the C_8 ssDNA would be extended toward the 3′ side of the duplex flank (stabilizing binding) (*6*), and preferential binding by hRPA would be observed to the Pyr/Pur-fork and 5′-Pyr-overhang substrates. In the second possibility where hRPA binds DNA with a 3′ → 5′ polarity, initial hRPA binding would extend in the 5′ direction, and hRPA would prefer binding the Pur/Pyr-fork and 3′-Pyr-overhang substrates. If hRPA does not bind DNA in a polar fashion, then no difference in hRPA binding to the Pyr/Pur- and Pur/Pyr-forks would be expected.

Of the four substrates that were tested, hRPA bound only to the Pyr/Pur-fork substrate at significant levels, although with reduced affinity as compared to the PO-8 bubble control (Figure 4A, lanes 1 and 2). Very weak binding was detected with the 5′-Pyr-overhang (lane 4), while no binding was observed to the Pur/Pyr-fork and 3′-Pyr-overhang substrates (lanes 3 and 5). The faster migrating hRPA-dependent bands observed in lanes 3 and 5 do not represent generated ssDNA, as indicated by comparison to ssDNA controls (not shown). It is possible that some atypical secondary structure of these substrates results in a pool of faster migrating species during native gel electrophoresis. hRPA binding to the fork and overhang substrates was also examined over a wider range of hRPA levels (Figure 4B). Although the presence of glutaraldehyde needed to observe the hRPA−DNA complexes prevents accurate determination of the binding constants, these data indicate that hRPA bound the Pyr/Pur-fork substrate with approximately 10-fold higher affinity than the Pur/Pyr-fork. Although the binding of hRPA to the 5′-Pyr-overhang substrate was weak, it was significantly stronger than the binding to the 3′-Pyr-overhang substrate. Overall, the selective binding of hRPA to the Pyr/Pur-fork indicates that the initial contact of hRPA with the arm fork is stabilized by extension of the protein onto the duplex flank in the 5′ → 3′ direction.

The binding of hRPA to both the Pyr/Pur-fork and 5′-Pyr-overhang substrates occurred with modified stoichiometry as compared to PO-8 bubble binding, as only hRPA monomers were formed (Figure 4A, compare lanes 2 and 4 with lane 1). The same stoichiometry was observed with two fork substrates containing cytosine (Pyr/Pyr-fork) or identical pyrimidine-rich (PO-8-fork) sequences on both fork arms (data not shown), even though these sequences supported oligomeric hRPA binding as part of pseudo-origin bubble substrates (see above). These results support our previous hypothesis that stable hRPA dimer formation on PO substrates occurs through cooperative hRPA binding across bubble strands (*6*).

The ability of hRPA to denature the fork and overhang substrates was examined. hRPA was not found to denature any of these four substrates, or the Pyr/Pyr- and PO-8-forks (data not shown). The lack of unwinding correlates with the noncooperative hRPA binding, suggesting that a single hRPA monomer cannot support efficient DNA denaturation. However, it is also possible that the longer contiguous DNA duplex in the fork and overhang substrates (40 bp) compared to the bubble molecules (which contain two 20 bp duplex flanks) prevents significant DNA unwinding.

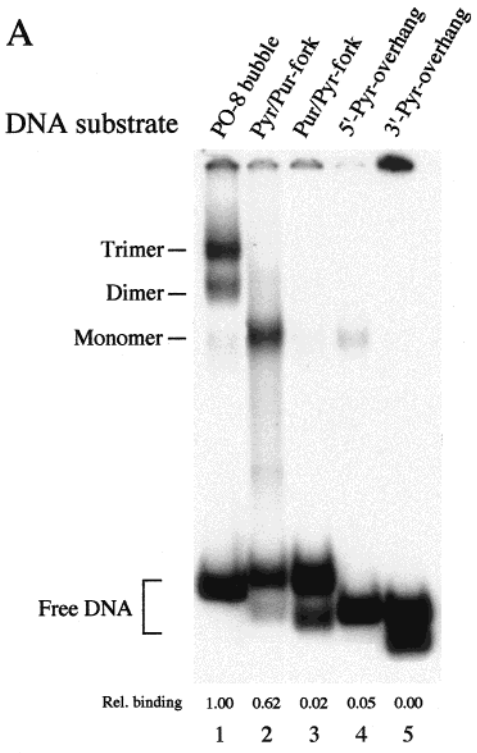

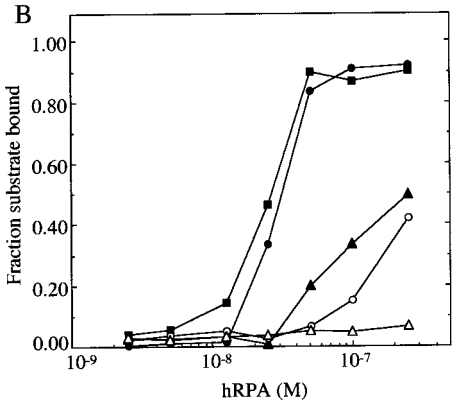

FIGURE 4: hRPA binding to both fork and overhang substrates occurs with a 5′ → 3′ polarity. (A) A constant amount of hRPA (1.5 pmol) was incubated with 0.15 pmol of each 5′-^{32}P-labeled DNA substrate, as indicated, under standard binding reaction conditions. The reaction products were then subjected to native gel electrophoresis and autoradiography. The positions of the hRPA complexes as well as the free DNA are shown. (B) Increasing amounts of hRPA (0.05−5 pmol) were incubated with 0.15 pmol of the 5′-^{32}P-labeled fork or overhang substrates under standard binding reaction conditions. The substrates that were used were the PO-8 fork (■), the Pyr/Pur-fork (●), the Pur/Pyr-fork (○), the 5′-Pyr-overhang (▲), and the 3′-Pyr-overhang (△). Reaction products were separated by native gel electrophoresis and autoradiography. Quantitation of the amount of substrate binding was performed as described in the legend of Figure 2. The fraction of each substrate bound is plotted as a function of the hRPA concentration.

Pseudo-Origin Binding and Unwinding by hRPA Are Dependent on the PO-8 Early Flank Sequence. As noted earlier, our data suggest that the efficiency of hRPA binding to pseudo-origin substrates is affected by the sequence of duplex flanks. Therefore, we directly examined the importance of the PO duplex flank sequence on the binding and unwinding activities of hRPA. Instead of randomly modifying the flank sequences, we designed four palindromic or inverse molecules derived from PO-8 (Figure 5). In the Early-Pal molecule, the entire late duplex flank was replaced with the early duplex flank, yielding a substrate with 2-fold symmetry. In the Early-Inv molecule (for Early-Inverse), the top strand of the late flank was replaced with the mirror image of the early flank top strand, basically scrambling the late flank sequence. The Late-Pal and Late-Inv substrates were constructed in a similar fashion. Each substrate has identical bubble sequences.

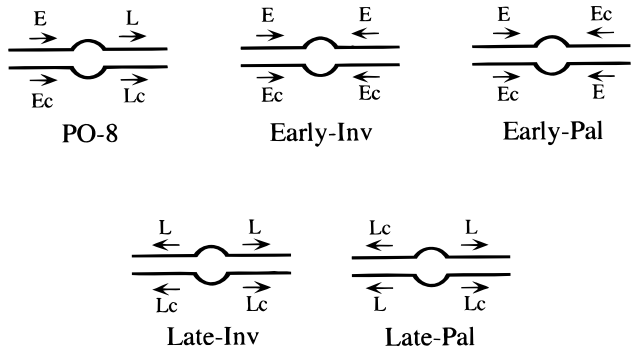

FIGURE 5: Pseudo-origin substrates used to test the effect of the duplex flank sequences on binding and unwinding by hRPA. Four palindromic or inverse PO substrates with modified early or late flank sequences were created. The Early-Inv substrate was designed to have the late PO-8 flank replaced with the mirror image of the early flank sequence, while Late-Inv contains the mirror image of the late sequence in place of the early flank. The Early-Pal substrate has the late sequence of the top (L) and bottom (Lc) strands replaced with the mirror image of the early bottom (Ec) and top (E) strand sequence, respectively. Similarly, the Late-Pal molecule contains the early top and bottom strand sequences replaced with the mirror images of the late bottom and top strand sequences, respectively. The latter two substrates thus have 2-fold symmetry with respect to the flanking duplex DNA. The bubble sequence for all four substrates is as described for PO-8 (see Experimental Procedures). The rightward arrows indicate the 5′ → 3′ sequence orientation, while the leftward arrows correspond to the 3′ → 5′ orientation.

With a single exception (Late-Inv), all substrates supported efficient binding and unwinding by hRPA, comparable to that observed with the PO-8 control (Figure 6A,B). Interestingly, the Late-Inv sequence was unable to support either hRPA activity (Figure 6A,B, lanes 8 and 9). These data indicate that, in addition to the sequence of the ssDNA bubble, the sequence composition of the PO duplex flanks is a critical determinant in supporting hRPA binding. As modification of only the early PO flank had significant effects on substrate binding and denaturation, these data could suggest that the early duplex flank sequence is a more critical determinant for hRPA recognition. Even so, replacement of the early flank with the late flank sequence in the Late-Pal molecule did not affect PO binding and unwinding (Figure 6A,B, lanes 5), suggesting that the natural sequence of both flanks facilitates hRPA interaction.

Effect of Different DNA Bending Sequences in the Early PO Flank. The early PO-8 flank contains a stretch of six adenosines on the top strand. In addition to being an important determinant for T antigen binding (*47*, *48*), adenosine runs can also introduce static bends into the DNA conformation (*49*). To test if DNA bending in the early flank affected the ability of hRPA to bind and unwind the pseudo-origin substrates, we constructed substrates in which the six top strand adenosines were replaced with various elements

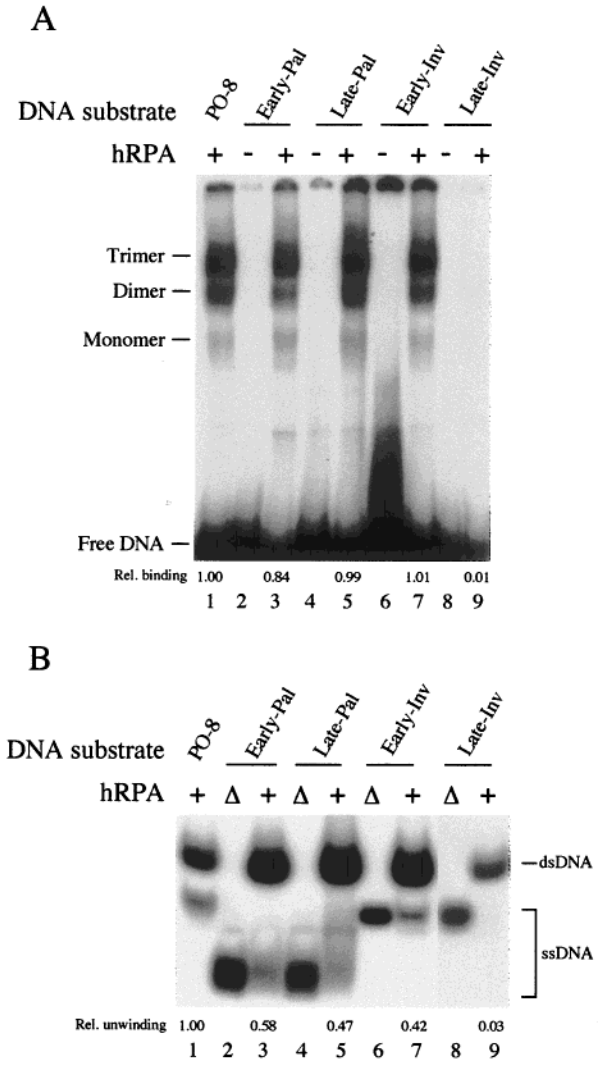

FIGURE 6: Effect of the duplex flank sequence on pseudo-origin binding and unwinding by hRPA. Each pseudo-origin substrate (0.15 pmol; 5′-^{32}P-labeled), as indicated (shown in Figure 5), was incubated with or without 1.5 pmol of hRPA under standard binding (A) and unwinding (B) reaction conditions. The reaction products were then separated by native gel electrophoresis and visualized by autoradiography. The identity of the generated ssDNA was established by comparison with the top strand of each substrate (Δ). The locations of hRPA−DNA complexes, the unbound PO substrate, and the duplex and single-stranded DNA forms of the substrates are shown. The level of substrate binding and unwinding was quantified as described in the legend of Figure 2.

(Figure 7). These were a T_6 element (TA-bend substrate), which would approximately maintain the same direction of bending (*50*); a G_3C_3 element (GC-bend substrate), which creates a flank with the opposite direction of bending (the G_3C_3 element causes a major groove compression as opposed to compression of the minor groove in the A_6 sequence) (*51*); and a C_3G_3 element (CG-control substrate), which does not form a stable bend (*52*). Note that current evidence strongly suggests that DNA bending is an intrinsic property arising from the dinucleotide or trinucleotide sequence, which would not be expected to be affected by a distal ssDNA bubble (*52*).

Somewhat surprisingly, when hRPA binding to these substrates was tested, only the PO-8 and GC-bend molecules were found to be efficiently bound (Figure 8A, lanes 1 and 5). Very weak binding was detected with both the TA-bend and CG-control substrates (lanes 3 and 7). In that the PO-8 and TA-bend substrates have an element that bends in the same direction, while the GC-bend molecule bends in the direction opposite from PO-8 (*52*, *53*), these observations indicate that bending of the early flank is not necessarily a requirement for high-affinity binding of hRPA to the pseudo-origin structure. Regardless, our data indicate that a feature of the early duplex centered one duplex turn from the proximal edge of the bubble can strongly modulate the ability of hRPA to bind the PO substrate.

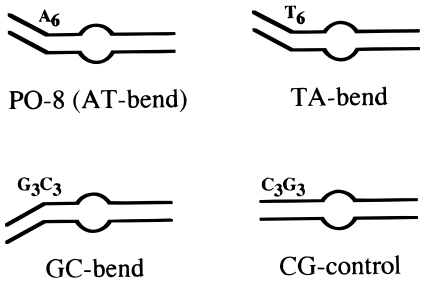

FIGURE 7: Pseudo-origin substrates used to test the effect of different DNA bending elements on hRPA binding and unwinding. Three pseudo-origin substrates with modified early flank sequences were constructed. The A_6 tract located on the top strand of the early PO-8 flank was replaced with six thymines (the TA-bend substrate), a G_3C_3 element (the GC-bend substrate), and a C_3G_3 tract that is not predicted to form a static bend (the CG-control substrate).

As expected, unwinding of both the TA- and CG-bend molecules was not observed (Figure 8B, lanes 3 and 7). Surprisingly, the GC-bend substrate was not denatured by hRPA, despite stable and cooperative binding of the protein (Figure 8A, lane 5). Although bending of the early flank does not seem to be critical for the hRPA binding activity, it is possible that this modified direction of bending in the G_3C_3 element creates a structural context that is unfavorable for unwinding of the GC-bend substrate by hRPA. Perhaps more likely, the increased thermal stability of the GC-bend substrate may prevent unwinding of this molecule by hRPA. Clearly, these results are in agreement with our previous hypothesis that complete unwinding of a PO molecule is not a prerequisite for stable hRPA binding (*7*).

Mutations of the Early Flank Region in the Ori Context Inhibit SV40 Ori Denaturation and DNA Replication. The pseudo-origin early flank contains auxiliary sequences (SV40 origin positions 5190−5210) that correspond to the T antigen binding site I (BS I) region (SV40 positions 5185−5210) (*47*, *54*). Although it has been shown that mutation of the BS I region decreases by several-fold the efficiency of SV40 DNA replication both in vitro and in vivo (*55*−*58*), the reduction in *ori* activity by certain mutations is apparently not a result of a loss of T antigen binding to site I (*56*, *58*). Thus, it is possible that a secondary role for the BS I region is to modulate *ori* activity by altering the affinity of hRPA for the 8 bp ssDNA element present in the T antigen−*ori* complex. Because the BS I region lies outside the minimal core *ori*, we tested this by examining the effect of BS I region mutations on *ori* denaturation and DNA replication in vitro.

The four early PO-8 bending derivatives were cloned adjacent to the core *ori* using spacing identical to that found in the pseudo-origin substrates and the SV40 *ori* region. To eliminate any effects of these mutations on T antigen binding to BS I, we modified this site at four nonconsecutive

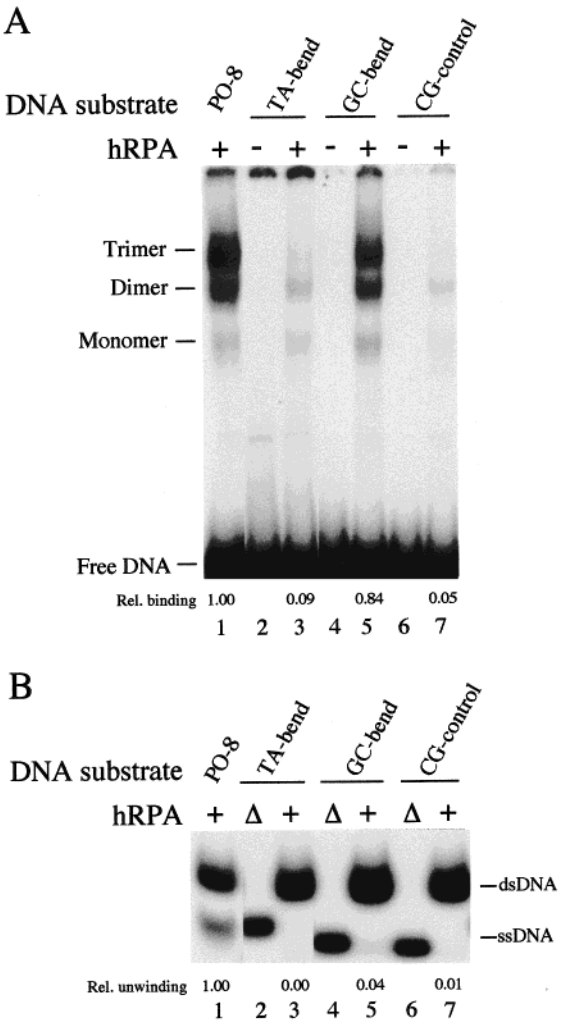

FIGURE 8: The pseudo-origin early flank contains a 6 bp region whose mutation modulates the binding and unwinding activities of hRPA. Each DNA substrate (0.15 pmol; 5′-^{32}P-labeled) was incubated with or without hRPA (1.5 pmol) at 37 °C, under standard binding (A) and unwinding (B) reaction conditions (see Experimental Procedures). For both binding and unwinding reactions, the reaction products were separated by native gel electrophoresis and visualized by autoradiography. The ssDNA controls (Δ) that were used were the 5′-^{32}P-labeled top strands of the pseudo-origin substrates. The positions of hRPA−DNA complexes, the unbound PO substrate, and the duplex and single-stranded DNA forms of the substrates are shown. The relative levels of substrate binding and unwinding are shown below the appropriate lanes in panels A and B, respectively.

positions to prevent T antigen binding (*47*). These same mutations do not affect binding and unwinding by hRPA when present in a pseudo-origin substrate (data not shown). In addition to the four plasmids containing the various bending elements in the context of a mutated BS I (pBS-ATmt, pBS-TAmt, pBS-GCmt, and pBS-CGmt), we also generated a plasmid that contained the wild-type BS I element (pBS-ATwt).

DNA fragments containing *ori* and the mutated BS I region were generated by PCR amplification. These DNA substrates were tested in an *ori* denaturation reaction in which T antigen and hRPA (or certain heterologous SSBs; *45*) catalyze the complete unwinding of *ori* in an ATP-dependent fashion (*20*). Using T antigen and hRPA, unwinding of the wild-type origin (*ori*-ATwt) was found to be slightly stimulated compared to that of *ori*-ATmt, the BS I-mutated control

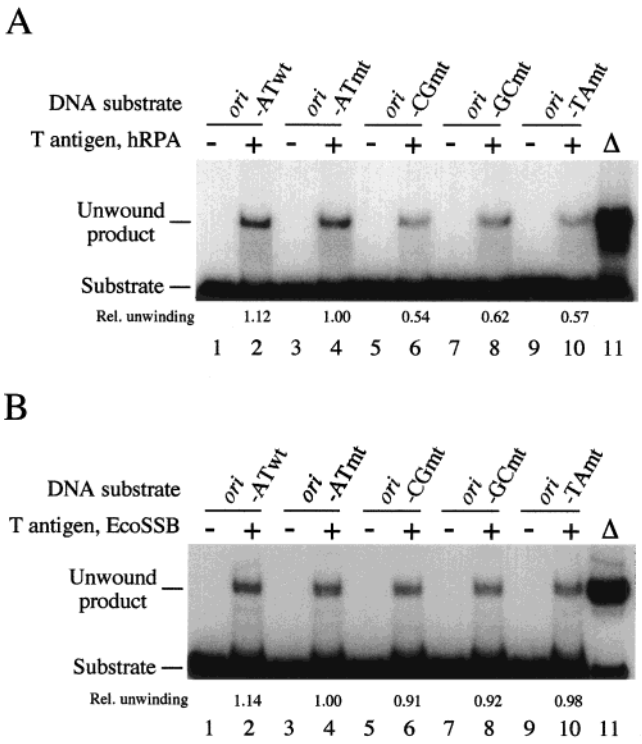

FIGURE 9: The effect of BS I region mutations on *ori* denaturation is specific for hRPA. Each ^{32}P-labeled *ori*-containing DNA fragment (100 fmol), as indicated, was incubated in the presence or absence of 1.0 μg of T antigen and 250 ng of either hRPA (A) or EcoSSB (B), for 1.5 h at 37 °C. The reaction products were separated by nondenaturing polyacrylamide gel electrophoresis and visualized by autoradiography. A marker lane showing a heat-denatured *ori*-ATwt substrate is also included (lane 11). The position of the duplex substrates and unwound products is indicated to the left of each panel. The fraction of DNA substrate unwound, normalized in each panel to the level found using the *ori*-ATmt substrate, was determined by densitometric analysis and is indicated below the appropriate lanes.

(Figure 9A). A significant reduction in *ori* activity was detected with *ori*-CGmt, *ori*-GCmt, and *ori*-TAmt substrates to levels between ~54 and 62% of that found with the *ori*-ATmt substrate. To verify that the consequences of the BS I region mutations were a result of altered hRPA interaction with *ori* rather than effects on the binding of T antigen to *ori*, we repeated the unwinding experiment using EcoSSB in place of hRPA (Figure 9B). In these reactions, each of the mutant *ori* substrates exhibited similar unwinding activities, although the extent of denaturation of the *ori*-GCmt and *ori*-CGmt substrates was found to be slightly reduced compared to that of *ori*-ATmt. These data indicate that the BS I region mutations can cause changes to *ori* activity that are a result of altered interactions of hRPA with this region.

Each mutant origin was also tested in the standard SV40 DNA replication assay in vitro (*43*) (Table 1). A pattern of origin activity similar to that found for *ori* denaturation using hRPA was observed. The *ori*-containing pBS-CGmt, pBS-GCmt, and pBS-TAmt plasmids were observed to be reduced to levels that were between 56 and 74% of the replication activity of pBS-ATmt. Thus, the DNA replication and denaturation activities of the mutant origins were found to correlate with the poor unwinding of the PO substrates containing the identical bending elements (see above).

As a point of comparison, we note that core *ori* substrates (lacking the BS I region) containing single point mutations

Table 1: SV40 DNA Replication Activity of Wild-Type and Mutant SV40 Origins[a]

SV40 origin plasmid	[^{3}H]dTTP incorporated in 2 h (pmol)	relative specific activity (%)
pBS-ATwt	38.6 ± 3.4	143
pBS-ATmt	27.0 ± 3.7	100
pBS-CGmt	19.9 ± 2.2	73.7
pBS-GCmt	19.5 ± 1.3	72.2
pBS-TAmt	15.2 ± 2.9	56.3

[a] SV40 replication reactions were performed by incubating 200 ng of each plasmid, 750 ng of T antigen, and 350 μg of HeLa replication extract in a standard replication mixture for 2 h at 37 °C. The amount of [^{3}H]dTTP incorporated in the newly synthesized DNA was determined by acid precipitation and scintillation counting. Three replication reactions per plasmid were carried out, and the average level of incorporation was determined. The relative in vitro replication efficiency of each mutant was defined as the amount of nucleotide incorporated into the mutant DNA expressed as a percentage of the amount of nucleotide incorporated into the pBS-ATmt DNA.

within the essential EP or AT-rich regions were previously found to have in vitro DNA replication activities (in crude extracts) that were an average of ~40% of that of the wild-type core *ori* (see Figure 3C of ref *11*). We therefore conclude that mutations which modulate the hRPA interaction with the BS I region can inhibit replication to a degree similar, if slightly reduced, to that of core *ori* mutations. Although significant, the effect of the early flank mutations on SV40 replication and *ori* denaturation is not as dramatic as the effect on hRPA binding. These data suggest that other stabilizing interactions, such as protein−protein contacts between T antigen and hRPA (*59*), may stimulate hRPA binding to the SV40 origin during replication and therefore partially compensate for the effect of the early flank mutations. Despite these differences, these results indicate that, aside from its role in T antigen binding, the BS I region contains an element that modulates the affinity of hRPA for *ori* during the initiation of SV40 DNA replication.

DISCUSSION

This study was undertaken to understand how DNA structure mediates the ability of hRPA to bind and unwind origin DNA elements during the initiation of eukaryotic DNA replication, using the SV40 model system. Our data reveal that hRPA binds with a 5′ → 3′ molecular polarity to the nascent bubble formed within the origin and suggest that this binding localizes the initiation sites of nascent strand synthesis to particular origin regions (see below). Moreover, our data indicate that hRPA activity and thus origin activity is modulated by the sequence of both ssDNA and dsDNA elements present in the origin initiation complex.

Our evidence for the 5′ → 3′ polarity of hRPA binding is based on the finding that hRPA has a strong preference for substrates that contain a 5′ pyrimidine arm (the Pyr/Pur-fork and 5′-Pyr-overhang) over substrates that contain a 3′ pyrimidine arm (the Pur/Pyr-fork and 3′-Pyr-overhang substrate). Because hRPA binds pyrimidine tracts more efficiently than purine tracts (Figure 2), and a duplex flank facilitates hRPA binding (*6*, *7*), these data indicate that the initial hRPA binding occurs to the ssDNA element, and this binding is then extended in the 3′ direction to contact the duplex flank. The possible criticism that the free 5′ or 3′ ssDNA end causes polar binding by hRPA which does not normally occur on internal ssDNA sites seems improbable for at least two reasons. First, the crystal structure of the primary ssDNA-binding domains complexed to an 8 nt ssDNA oligonucleotide showed that this domain bound the DNA with a particular polarity, but no specific contacts to the DNA ends were apparent (*37*). Second, we found that hRPA binding to the fork and overhang substrates had a similar preference for pyrimidine-rich over purine-rich DNA as was found for both PO and completely ssDNA substrates. One would have to propose a more complex hypothesis in which hRPA uses different binding mechanisms to bind DNA ends and internal ssDNA regions, yet is similarly modulated by oligonucleotide composition, a proposal we consider unlikely.

As this work was in progress, de Laat et al. demonstrated a 5′ → 3′ molecular polarity of hRPA binding in conjunction with its role in the nucleotide excision repair process (*60*). Using self-complementary oligonucleotides with either 3′ or 5′ ssDNA overhangs, this group found that hRPA bound preferentially to a 19 nt 3′ overhang. These results were interpreted to show that hRPA contained a strong ssDNA-binding entity on the 5′ portion of the bound ssDNA, and a weaker ssDNA-binding region to the 3′ side of the strong site. In that we find that use of shorter (8 nt) arms results in preferential binding of hRPA to 5′ overhangs (Figure 4), these data indicate that hRPA can use the flanking duplex DNA to stabilize binding when short (~8 nt) ssDNA regions are available. With increases in the ssDNA length, the duplex DNA serves to inhibit hRPA binding and causes a switch of preferential hRPA binding from a 5′ overhang to a 3′ overhang.

In the context of the SV40 T antigen−*ori* complex, our data indicate that hRPA binding involves initial interaction with the ssDNA bubble region, with this binding being stabilized by cooperative interactions between an hRPA molecule bound to each strand (Figure 10; *6*). Because extension of the binding site proceeds in the 5′ → 3′ direction, these data suggest that the hRPA molecule bound to the top strand would interact with DNA sequences within the core origin to the right of position 5210. Similarly, the hRPA molecule bound to the bottom strand would interact with sequences normally to the left of the core *ori*, including BS I (i.e., to the left of SV40 position 5217). The interaction of hRPA with the duplex DNA flanks leads to their destabilization, and the subsequent enlargement of the bubble region. As proposed previously (*6*), the denaturation of the duplex DNA within the core *ori* destroys the T antigen recognition element, releasing the T antigen DNA helicase to unwind the DNA outward from the origin.

The identification of multiple RPA DBDs (*25*, *33*−*40*) can be correlated with the proposed molecular polarity of hRPA binding to the PO substrate. That is, the initial contact of the hRPA monomer with the bubble may occur through the central high-affinity DBDs A and B to form the $hRPA_{8nt}$ complex. In this model, conversion to the $hRPA_{30nt}$ complex would involve additional interaction with the pseudo-origin duplex flanks via one or both of the secondary DBDs (DBD C and DBD D), resulting in a 5′ to 3′ extended orientation of each hRPA monomer onto the DNA. Thus, the secondary DBDs contact the DNA in a 3′ direction from the initial binding of the primary DBD.

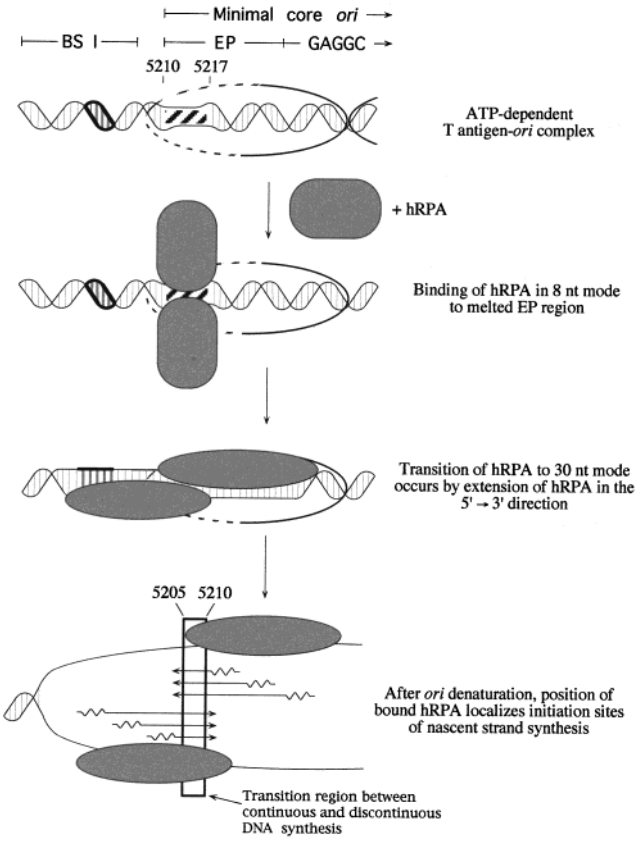

FIGURE 10: Model of polar hRPA binding to the T antigen−*ori* complex. As described in greater detail in the text, T antigen binds in the presence of ATP to form a double-hexameric complex over the minimal core *ori*, including the EP and the central GAGGC element (only the early half of the *ori* complex is shown). A molecule of hRPA binds (in the $hRPA_{8nt}$ mode) to each strand of the 8 nt EP bubble (SV40 positions 5210−5217), with the binding being stabilized by cooperative interactions across both strands. hRPA then undergoes a conformational transition to the $hRPA_{30nt}$ complex, with each molecule extending in the 5′ → 3′ direction. Binding of the bottom hRPA molecule to the duplex DNA is facilitated by an element present in the BS I region (shown by a bold region of DNA). After complete denaturation of *ori* (the position of the T antigen helicase not shown), the initiation sites of nascent strand synthesis are localized by the position of the bound hRPA. The boxed region in the bottom panel indicates the transition region between continuous and discontinuous DNA synthesis found to occur in vivo at SV40 positions ∼5205−5210 (*61*, *62*).

Importantly, mapping of the SV40 initiation sites for nascent strand synthesis in vivo showed a transition between continuous and discontinuous DNA synthesis in the region corresponding to SV40 positions 5205−5210 (*61*, *62*). That is, the initiation of leading strand synthesis moving in the early gene direction (to the left from *ori* as drawn in Figure 10) was observed to the right of the transition region, while the initiation of leading strands moving toward the late genes (to the right) was found to the left of the transition region. As the mammalian DNA primase initiates nascent strand synthesis with an ∼10 nt RNA primer (*63*, *64*), the initiation region for leading strand synthesis moving in both directions closely corresponds to proposed sites of hRPA binding on both strands. Because hRPA is known to stimulate human primase under certain conditions (*65*, *66*), we propose that the bound hRPA facilitates binding of the DNA polymerase α−DNA primase complex, thus localizing the initiation of replication to particular sites. We note that the yeast ARS1 origin also contains a transition region for continuous and discontinuous DNA synthesis when located either on a plasmid or at its natural chromosomal location (*62*, *67*). We speculate that the location of scRPA binding to the nascent bubble within the ARS1 initiation complex also positions the initiation sites for this chromosomal origin.

We found that replacement or mutation of the early flank of the PO-8 substrate (e.g., the Late-Inv, TA-bend, and CG-control substrates) drastically affected both hRPA binding and unwinding. This region was also found to play a modulatory role in SV40 DNA replication (see below). Although the early flank contains an A_6 bending element (at SV40 positions 5198−5203), we found no correlation between the direction of DNA bending and the ability to support hRPA binding. In addition, there is no other obvious correlative feature of those sequences which support hRPA binding (A_6 and G_3C_3) as opposed to those which bind hRPA poorly (T_6, C_3G_3, and TCGATA; the latter sequence in the Late-Inv substrate) other than the presence of three 5′ purines. As this element is centered one duplex turn from the proximal edge of the bubble, it is possible that indirect effects of the element on the structure of the sugar−phosphate backbone modulate the ability of hRPA to bind (indirect readout; *68*−*70*). Regardless, our data indicate that the region of positions 5198−5203 contains an element that affects hRPA binding both in the context of the PO substrate and in the natural SV40 *ori* region.

As a structural element providing the entry site for the interaction of hRPA with the PO substrates, we find that the ssDNA bubble sequence composition is an important determinant of the initial recognition of the PO substrate by hRPA. The selective binding of hRPA to pyrimidine bubbles confirms previous reports describing RPA as preferring pyrimidine-rich sequences (*29*, *71*). With six pyrimidines out of eight nucleotides on each strand of the bubble, the PO-8 substrate closely resembles a Pyr/Pyr-bubble molecule. Because the top strand bubble sequence of the PO-8 substrate is identical to that of *ori*, these data suggest that, during the initiation of SV40 DNA replication, the first molecule of hRPA binds to the top strand of the melted EP element. Interestingly, our data suggest that the BS I region, which would interact with the hRPA molecule bound to the bottom strand (see above), contains an A_6 element that supports PO binding and unwinding by hRPA. We therefore postulate that the weaker binding of hRPA to the bottom strand (purine-rich) ssDNA element in the T antigen−*ori* complex is stabilized by the early flank element.

Changes to the BS I region at positions 5198−5203 were found to significantly affect SV40 DNA replication (Table 1). *Ori* denaturation experiments indicate that the modulatory effects are due to an interaction of hRPA with the BS I region. As the BS I region was also mutated to prevent T antigen binding, these data rule out any effect of the early flank elements on *ori* activity through T antigen−BS I complex formation. Because we find that the level of hRPA unwinding of the PO substrates generally correlates with SV40 replication efficiency, our data suggest that the BS I sequence can also affect *ori* activity through its ability to assist denaturation of these elements by hRPA. Interestingly, investigation of the BS I region has previously led to the suggestion that it could increase *ori* activity in a manner independent of T antigen binding to BS I (*56*, *58*). Thus,

the BS I region can modulate the initiation of SV40 replication by multiple mechanisms, including facilitating hRPA binding. More generally, our data indicate that the activity of eukaryotic origins can be regulated by the presence of discrete cis-acting elements that alter the ability of RPA to bind and unwind origin sequences.

ACKNOWLEDGMENT

We thank Mehboob Shivji for assistance in the *ori* cloning experiments, D. Goodsell for discussions on DNA bending, M. Dlakic for use of the DIAMOD program to model the DNA bending of our PO substrates, and Yaron Daniely for critical reading of the manuscript.

REFERENCES

1. Baker, T. A., Sekimizu, K., Funnell, B. E., and Kornberg, A. (1986) *Cell 45*, 53−64.
2. Dodson, M., Echols, H., Wickner, S., Alfano, C., Mensa-Wilmot, K., Gomes, B., LeBowitz, J., Roberts, J. D., and McMacken, R. (1986) *Proc. Natl. Acad. Sci. U.S.A. 83*, 7638−7642.
3. Dean, F. B., Bullock, P., Murakami, Y., Wobbe, C. R., Weissbach, L., and Hurwitz, J. (1987) *Proc. Natl. Acad. Sci. U.S.A. 84*, 16−20.
4. Wold, M. S., Li, J. J., and Kelly, T. J. (1987) *Proc. Natl. Acad. Sci. U.S.A. 84*, 3643−3647.
5. Iftode, C., Daniely, Y., and Borowiec, J. A. (1999) *Crit. Rev. Biochem. Mol. Biol. 34*, 141−180.
6. Iftode, C., and Borowiec, J. A. (1997) *Mol. Cell. Biol. 17*, 3876−3883.
7. Iftode, C., and Borowiec, J. A. (1998) *Nucleic Acids Res. 26*, 5636−5643.
8. Deb, S., DeLucia, A. L., Baur, C.-P., Koff, A., and Tegtmeyer, P. (1986) *Mol. Cell. Biol. 6*, 1663−1670.
9. Deb, S., DeLucia, A. L., Koff, A., Tsui, S., and Tegtmeyer, P. (1986) *Mol. Cell. Biol. 6*, 4578−4584.
10. Deb, S., Tsui, S., Koff, A., DeLucia, A., Parsons, R., and Tegtmeyer, P. (1987) *J. Virol. 61*, 2143−2149.
11. Dean, F., Borowiec, J., Ishimi, Y., Deb, S., Tegtmeyer, P., and Hurwitz, J. (1987) *Proc. Natl. Acad. Sci. U.S.A. 84*, 8267−8271.
12. Dean, F. B., Dodson, M., Echols, H., and Hurwitz, J. (1987) *Proc. Natl. Acad. Sci. U.S.A. 84*, 8981−8985.
13. Deb, S., and Tegtmeyer, P. (1987) *J. Virol. 61*, 3649−3654.
14. Borowiec, J. A., and Hurwitz, J. (1988) *Proc. Natl. Acad. Sci. U.S.A. 85*, 64−68.
15. Mastrangelo, I. A., Hough, P. V. C., Wall, J. S., Dodson, M., Dean, F. B., and Hurwitz, J. (1989) *Nature 338*, 658−662.
16. Parsons, R. E., Stenger, J. E., Ray, S., Welker, R., Anderson, M. E., and Tegtmeyer, P. (1991) *J. Virol. 65*, 2798−2806.
17. Borowiec, J. A., and Hurwitz, J. (1988) *EMBO J. 7*, 3149−3158.
18. Parsons, R., Anderson, M. E., and Tegtmeyer, P. (1990) *J. Virol. 64*, 509−518.
19. Stahl, H., Dröge, P., and Knippers, R. (1986) *EMBO J. 5*, 1939−1944.
20. Goetz, G. S., Dean, F. B., Hurwitz, J., and Matson, S. W. (1988) *J. Biol. Chem. 263*, 383−392.
21. Wiekowski, M., Schwarz, M. W., and Stahl, H. (1988) *J. Biol. Chem. 263*, 436−442.
22. Brill, S. J., and Stillman, B. (1989) *Nature 342*, 92−95.
23. Smelkova, N. V., and Borowiec, J. A. (1997) *J. Virol. 71*, 8766−8773.
24. Smelkova, N. V., and Borowiec, J. A. (1998) *J. Virol. 72*, 8676−8681.
25. Lao, Y., Lee, C. G., and Wold, M. S. (1999) *Biochemistry 38*, 3974−3984.
26. Blackwell, L. J., and Borowiec, J. A. (1994) *Mol. Cell. Biol. 14*, 3993−4001.
27. Blackwell, L. J., Borowiec, J. A., and Mastrangelo, I. A. (1996) *Mol. Cell. Biol. 16*, 4798−4807.
28. Lavrik, O. I., Nasheuer, H.-P., Weisshart, K., Wold, M. S., Prasad, R., Beard, W. A., Wilson, S. H., and Favre, A. (1998) *Nucleic Acids Res. 26*, 602−607.
29. Kim, C., Snyder, R. O., and Wold, M. S. (1992) *Mol. Cell. Biol. 12*, 3050−3059.
30. Seroussi, E., and Lavi, S. (1993) *J. Biol. Chem. 268*, 7147−7154.
31. Kim, C., Paulus, B. F., and Wold, M. S. (1994) *Biochemistry 33*, 14197−14206.
32. Gomes, X. V., Henricksen, L. A., and Wold, M. S. (1996) *Biochemistry 35*, 5586−5595.
33. Gomes, X. V., and Wold, M. S. (1996) *Biochemistry 35*, 10558−10568.
34. Kim, D.-K., Stigger, E., and Lee, S.-H. (1996) *J. Biol. Chem. 271*, 15124−15129.
35. Lin, Y.-L., Chen, C., Keshav, K. F., Winchester, E., and Dutta, A. (1996) *J. Biol. Chem. 271*, 17190−17198.
36. Philipova, D., Mullen, J. R., Maniar, H. S., Lu, J., Gu, C., and Brill, S. J. (1996) *Genes Dev. 10*, 2222−2233.
37. Bochkarev, A., Pfuetzner, R. A., Edwards, A. M., and Frappier, L. (1997) *Nature 385*, 176−181.
38. Brill, S. J., and Bastin-Shanower, S. (1998) *Mol. Cell. Biol. 18*, 7225−7234.
39. Bochkareva, E., Frappier, L., Edwards, A. M., and Bochkarev, A. (1998) *J. Biol. Chem. 273*, 3932−3936.
40. Sibenaller, Z. A., Sorensen, B. R., and Wold, M. S. (1998) *Biochemistry 37*, 12496−12506.
41. Henricksen, L. A., Umbricht, C. B., and Wold, M. S. (1994) *J. Biol. Chem. 269*, 11121−11132.
42. Borowiec, J. (1992) *J. Virol. 66*, 5248−5255.
43. Wobbe, C. R., Dean, F., Weissbach, L., and Hurwitz, J. (1985) *Proc. Natl. Acad. Sci. U.S.A. 82*, 5710−5714.
44. Borowiec, J. A., Gillette, T. G., Smelkova, N. V., and Iftode, C. (1999) in *Eukaryotic DNA replication: A practical approach* (Cotterill, S., Ed.) pp 245−273, Oxford University Press, Oxford.
45. Kenny, M. K., Lee, S.-H., and Hurwitz, J. (1989) *Proc. Natl. Acad. Sci. U.S.A. 86*, 9757−9761.
46. Lavrik, O. I., Kolpashchikov, D. M., Nasheuer, H. P., Weisshart, K., and Favre, A. (1998) *FEBS Lett. 441*, 186−190.
47. Ryder, K., Vakalopoulou, E., Mertz, R., Mastrangelo, I., Hough, P., Tegtmeyer, P., and Fanning, E. (1985) *Cell 42*, 539−548.
48. Ryder, K., Silver, S., DeLucia, A. L., Fanning, E., and Tegtmeyer, P. (1986) *Cell 44*, 719−725.
49. Wu, H. M., and Crothers, D. M. (1984) *Nature 308*, 509−513.
50. Koo, H. S., and Crothers, D. M. (1988) *Proc. Natl. Acad. Sci. U.S.A. 85*, 1763−1767.
51. Brukner, I., Susic, S., Dlakic, M., Savic, A., and Pongor, S. (1994) *J. Mol. Biol. 236*, 26−32.
52. Goodsell, D. S., and Dickerson, R. E. (1994) *Nucleic Acids Res. 22*, 5497−5503.
53. Dlakic, M., and Harrington, R. E. (1998) *Bioinformatics 14*, 326−331.
54. Tjian, R. (1978) *Cell 13*, 165−179.
55. DeLucia, A. L., Deb, S., Partin, K., and Tegtmeyer, P. (1986) *J. Virol. 57*, 138−144.
56. Li, J. J., Peden, K. W. C., Dixon, R. A., and Kelly, T. (1986) *Mol. Cell. Biol. 6*, 1117−1128.
57. Guo, Z. S., Gutierrez, C., Heine, U., Sogo, J. M., and Depamphilis, M. L. (1989) *Mol. Cell. Biol. 9*, 3593−3602.
58. Gutierrez, C., Guo, Z.-S., Roberts, J., and DePamphilis, M. L. (1990) *Mol. Cell. Biol. 10*, 1719−1728.
59. Dornreiter, I., Erdile, L. F., Gilbert, I. U., von Winkler, D., Kelly, T. J., and Fanning, E. (1992) *EMBO J. 11*, 769−776.
60. de Laat, W. L., Appeldoorn, E., Sugasawa, K., Weterings, E., Jaspers, N. G. J., and Hoeijmakers, J. H. J. (1998) *Genes Dev. 12*, 2598−2609.
61. Hay, R. T., and DePamphilis, M. L. (1982) *Cell 28*, 767−779.
62. Bielinsky, A. K., and Gerbi, S. A. (1998) *Science 279*, 95−98.

63. Yagura, T., Kozu, T., and Seno, T. (1982) *J. Biol. Chem. 257*, 11121−11127.
64. Tseng, B. Y., and Ahlem, C. N. (1983) *J. Biol. Chem. 258*, 9845−9849.
65. Matsumoto, T., Eki, T., and Hurwitz, J. (1990) *Proc. Natl. Acad. Sci. U.S.A. 87*, 9712−9716.
66. Melendy, T., and Stillman, B. (1993) *J. Biol. Chem. 268*, 3389−3395.
67. Bielinsky, A. K., and Gerbi, S. A. (1999) *Mol. Cell 3*, 477−486.
68. Drew, H. R., and Travers, A. A. (1985) *Nucleic Acids Res. 13*, 4445−4467.
69. Otwinowski, Z., Schevitz, R. W., Zhang, R. G., Lawson, C. L., Joachimiak, A., Marmorstein, R. Q., Luisi, B. F., and Sigler, P. B. (1988) *Nature 335*, 321−329.
70. Lesser, D. R., Kurpiewski, M. R., and Jen-Jacobson, L. (1990) *Science 250*, 776−786.
71. Carmichael, E. P., Roome, J. M., and Wahl, A. F. (1993) *Mol. Cell. Biol. 13*, 408−420.

BI0005761